Fuel Vapor Concentration Measurements By Infra-Red Extinction – Development Around A Mono Disperse Droplet Stream – ICLASS2009-085

B.Wagner* [1), 2)], P.Gajan[2)] and A.Strzelecki[2)]

[1] CERFACS, 42 av. Gaspard Coriolis, 31057 Toulouse, France
[2] Department of Aerodynamic and Energetic Modeling
Office National d'Etudes et de la Recherche Aéronautique (ONERA)
2, Edouard Belin, 31055 Toulouse, France

Abstract

A Two-Wavelength Infra-Red Extinction Technique (IRE) at 3392 and 632.8 nm is applied on a stream of monodisperse droplets to investigate the behavior of this technique in a small-scale environment with strong concentration gradients.

First, a brief excurse in the theory of Infra-Red absorption is done and the experimental setup is presented. Then, first results compared to a simplified numerical calculation are presented. These prove the general aptitude of the IRE for this type of application. Sources of error are analyzed and strategies to refine the results are developed. Two of these strategies concerning the simulation are presented and their potential of amelioration is estimated. Finally the results are discussed and perspectives of the work are given.

Introduction

Considering the current situation of increasing worldwide traffic and the rapid diminution of natural resources, the optimization of combustion processes is a top-priority, both environmentally and economically. A key factor for improvements in the efficiency of combustion chambers is the knowledge of local equivalent ratios, thus fuel concentrations. The objective of this study is the characterization of these local values.

Today, one of the most commonly used measurement techniques to validate evaporation calculations is (Planar) Laser Induced Fluorescence (PLIF). The advantages of this method are its ability to obtain instantaneous 2D concentration images and to detect several species by tuning the laser wavelength. However, the strong concentration (and thus fluorescence) gradients between liquid and vapor phase cause a "blooming" effect in the vicinity of the interface, making it impossible to obtain exact results in this region(see figure 1). To overcome this loss of information, a complementary measurement technique is desirable. IRE was chosen due to its capability to deal with sudden changes of concentration, low-energy consumption, therefore reduced material cost and the ability to perform measurements at high repetition rates. Since its development in the nineteen-seventies many investigations on static and pulsating configurations were realized [1-3]. However, no application to the liquid-gas interface nor comparisons to other non-intrusive concentration measurements such as (P)LIF are known to the authors. This paper describes the application of the IRE on a monodisperse stream and the difficulties encountered. It has to be noted, that this work is in progress and that comparative results to the PLIF measurements done earlier have been delayed after the due date of this paper, but shall be presented in future publications.

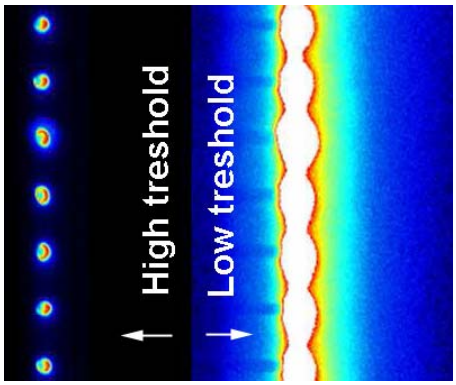

Figure 1: Blooming at a droplet stream

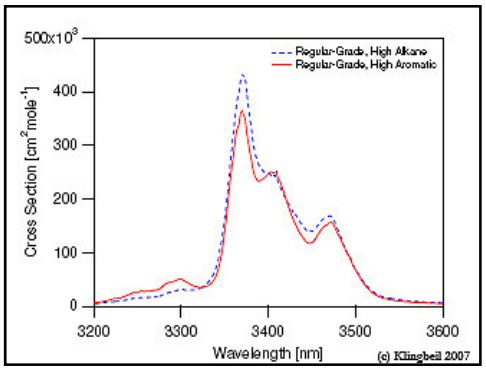

Figure 2: Absorption spectrum of gasoline

* Corresponding Author

Theory of the IRE

The Infrared Extinction Method is based on the ability of molecules to absorb energy through transition between its vibrational or rotational levels. It is important to mention, that this is a simple conversion of radiation energy into kinetic energy (thus heat) without any emission of radiation like for fluorescence techniques. In case of hydrocarbons, a strong absorption band can be found in the infrared regime at 3.39 µm (2945 cm^{-1}) [4,5]. Figure 2 gives an example of the absorption spectrum for standard gasoline. Hence a 3.39 µm monochromatic laser beam will experience a significant loss of intensity in gasoline vapor while an other beam of different wavelength will be affected very little or not at all.
The energy transmitted through a medium having a constant vapor concentration c_m follows the Beer-Bouguer-Lambert law:

$$\frac{I_{(x)}}{I_0} = e^{-\overbrace{\int_0^x \alpha_{(\lambda,P,T)} \cdot c_{m(x)} \cdot dx}^{K_{vapor}}} \tag{1}$$

Knowing the length of the crossed area x and the specific absorption coefficient for the ambient conditions $\alpha_{(\lambda,P,T)}$, the concentration c_m is easily determined. It has to be mentioned, that this value for K_{vapor} is an integral over the full line of sight. To achieve point results, deconvolution procedures have to be applied. Additionally, (1) is only valid in a homogeneous one-phase environment. When applied to a multi-phase flow the right hand side of the equation has to be replaced by several coefficients, taking into consideration the number of phases:

$$\frac{I}{I_0} = exp\,[-K_{drop-scat}] \cdot exp\,[-K_{drop-abs}] \cdot exp\,[-K_{vapor}] \tag{2}$$

Equation (2) shows the extension corresponding to the investigated test case using a stream of monodisperse droplets. Apart from vapor extinction, a significant part of the extinction origins in the presence of the liquid.
Since the goal is to measure the extinction due to the vapor phase the problem shifts to determine the drop-related components. This can be done by the use of a second laser beam emitting at a non-absorbing - for example, visible - wavelength:

$$\frac{I}{I_0} = \overbrace{\underbrace{exp[-K_{drop-scat}]}_{visible} \cdot \underbrace{exp[-K_{drop-abs}]}_{\ll 1} \cdot exp[-K_{vapor}]}^{Infra-Red} \tag{3}$$

Assuming that the influence of the droplets is independent of the wavelength, equation (2) can be simplified to:

$$K_{vapor} = \ln\left(\frac{I}{I_0}\right)_{vis} - \ln\left(\frac{I}{I_0}\right)_{IR} \tag{4}$$

The above assumption of equal drop optical thickness for both wavelengths – originally shown for sprays with an Area Mean Diameter ≥ 20 µm by J.A.Drallmeier [6] - was verified for the present experimental setup by a geometrical optics calculation. This calculation shows, that for both wavelengths over 95% of the laser light entering in the droplet are refracted in a way that they don't reach the collimating lens, and thus the sensors, anymore. This effect makes the droplet appear as an 'intensity hole' for the sensor, reducing the wavelength-dependent difference in liquid absorption to a negligible magnitude.

Experimental Setup and Post-processing Routines

The piezo-ceramic injector (see figure 3) is the centerpiece the setup presented in this paper. It is based on the Rayleigh disintegration of the liquid and provides a stream of calibrated droplets with the same size, velocity, temperature and spacing parameter $C = S_g/D_g$ at a given distance from the orifice. Therefore measurements at different positions result in a temporal evolution of a considered droplet in the jet. All presented results were acquired in a distance from 35 to 50*[mm]* from the orifice. The spacing parameter is set to comply with the frequency of the ceramic. Mass flow rate conservation yields the droplet diameter depending on the orifice and the pressure of the liquid. For the experimental conditions used, the decrease of the droplet size in the stream due to evaporation was calculated to be small in comparison to the diameter. Therefore it is considered negligible [7].

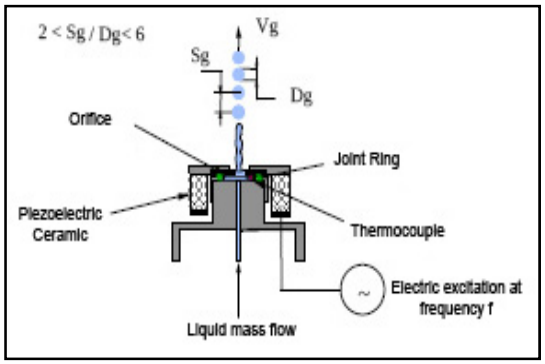

Figure 3: Injector principle

Two-wavelength Infra-Red Extinction is a line of sight measurement technique (see figures 4 and 5). The laser-beams, one at 3.392*[μm]* and 2*[mW]* (Infra-Red) and the other at 632.8*[nm]* and 5*[mW]* (red-visible) are superposed by the aid of a dichroic mirror. Before passing the experimental area the beam widths are matched by a pinhole of 1 mm diameter which also ensures a good approximation of a Gaussian beam energy distribution. A second dichroic mirror acts as beam splitter and directs the beams to their respective photo-detectors. The visible detector is a Si-Type detector with an output signal of 0.42*[A/W]* and an optimal spectral range from 600 to 900*[nm]*. For acquisition of infrared radiation a PbSe-detector Type is employed. Its output signal reaches a maximum at an optimal wavelength range between 3 and 3.7*[μm]*. Both detectors are shielded from scattered light by pinholes mounted directly in front of them. The outgoing signals are preamplified before entering the PC-based acquisition chain.
To enhance temporal resolution a Chopper is placed between the experimental area and the beam splitter. This

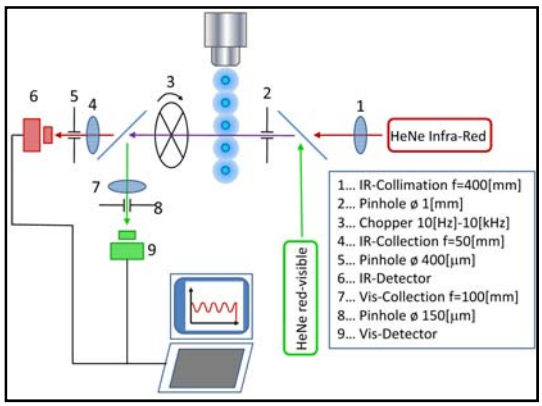

Figure 4: schematic IRE setup

Figure 5: Photograph of the IRE setup

creates a rectangular signal at a well defined frequency acting as the main reference for the synchronization of the system.
Suggestions for the focal lengths of the employed lenses as well as for the diameters of the pinholes were taken from the works of Hassa et al.[8].

Since the IRE is an integral line-of-sight measurement technique, calibration is limited to obtain the molar absorption coefficient and signal deformations due to the electrical components. The former can easily be achieved by measuring the Laser intensity diminution by a closed cell with known dimension, temperature, pressure and vapor concentration. Given that such measurements were already performed for acetone under the ambient conditions of

our setup [9], the value of $\alpha = 1.1 \cdot 10^4 [cm^2/mol]$ is known to suit to the ambient conditions and was adopted for the present work.

The latter is done by the aid of a calibration measurement run without droplet stream, leaving only systematic influences on the signal. Those are separated and subtracted from the measurement run signal.

As described, the IRE acquisition chain provides the signals of the visible and the IR channel in chopped, thus rectangular form. Figure 6 illustrates their post processing in order to identify the signal of a single representative droplet:

After eliminating temporal energy fluctuations by averaging all of the chopper periods (top left → top right) a correction of the noise as well as of the systematic deformations is effectuated (top right → bottom left). This is a crucial step in post processing since these deformations are of the same magnitude than the extinction induced by a single droplet (≈ 3-4% of the signal amplitude). The filtered droplet signals - distinguishable as small, periodic diminutions of the positive signal flank - are again averaged to obtain a mean droplet passing (bottom left → bottom right).

This Gaussian-like shape represents the extinction of the laser energy by a droplet and its surrounding vapor field crossing the laser beam. To identify the extinction due to the vapor field, the averaged contribution of the liquid phase detected by the visible channel is subtracted from the Infra-Red one, following equation (4).

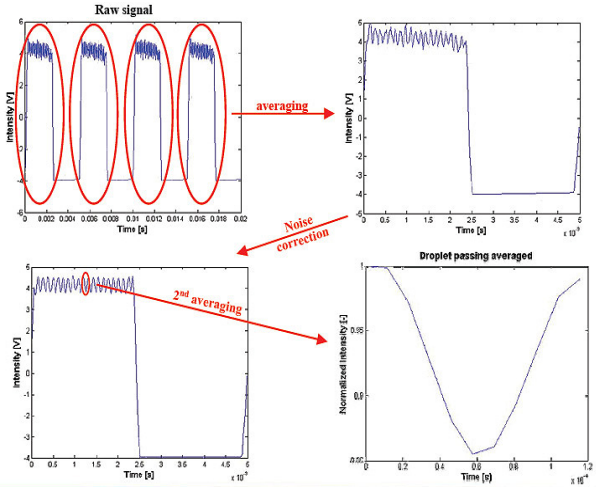

Figure 6: droplet post-processing

Simplified model

Since the resulting vapor-absorption profile consists of line-of-sight integrated values, a vapor mole fraction profile cannot be directly developed from one measurement. A.R.Chraplyvy proposes to combine the results of multiple measurements at slightly varying positions of laser beam and vapor field to obtain local concentration values by using an Onion-Peeling-Approach [2]. The aim was, to compare these values to the existing PLIF results. Unfortunately, if the laser beam diameter is not significantly smaller than the vapor field to be investigated, both the field and the Gaussian beam have to be segmented. This leads to costly 3D calculations to obtain the true amount of energy absorbed. Thus, this approach was found to be unsuitable for the present experimental configuration. In consequence, to validate the experimental results, a simplified numerical calculation was performed. The model consists in a calculation of the laser beam absorption by the vapor around a static, isolated and spherical droplet. This droplet and the surrounding vapor field are considered to be isothermal. The vapor mass fraction in the vicinity of the droplet, μ, is described by the following analytical expression, with μ_s being its saturated value and D_g indicating the droplet diameter. x and y are Cartesian coordinates originating in the droplet center:

$$\mu_{x,y} = 1 + (\mu_s - 1) \cdot exp\left[\left(1 - \frac{D_g}{2 \cdot \sqrt{x^2+y^2}}\right) \cdot \ln\left(1 + \frac{\mu_s}{1-\mu_s}\right)\right] \qquad (5)$$

The laser beam is considered to be cylindrical with a fixed diameter and its initial radial energy profile follows a Gaussian law. To simulate the interaction of the laser beam with a moving droplet, different respective positions were calculated. For each position, the resulting output energy of the laser beam is obtained from the integration of the energy profile calculated after its interaction with the droplet area.

Analysis of the simplified approach

Figure 7 shows a comparison of the calculated absorption by the vapor field of a droplet Dg = 246$[\mu m]$, ambient temperature) passing the laser beams, and the experimental result for the respective case. The latter was calculated from the difference between the mean droplet passages of the IR and the visible channel, following equation (4).

While magnitudes of the amplitudes, and thus the absorption, resemble (± 1% of total absorption), there is a significant difference in the shape and width of the signals. This can be explained by several facts:

- The main difference lies in the fact that the calculation simulates an isolated, static droplet with a well developed vapor field being crossed by a laser beam. In the experiment however it is the opposite way: The droplets cross the laser beam, forming a vapor 'tunnel'. Since the beam width is smaller and the tunnel creates a more homogeneous distribution than a developed vapor field, the experimental signal is narrower. A change to a more realistic model is described in the next section.

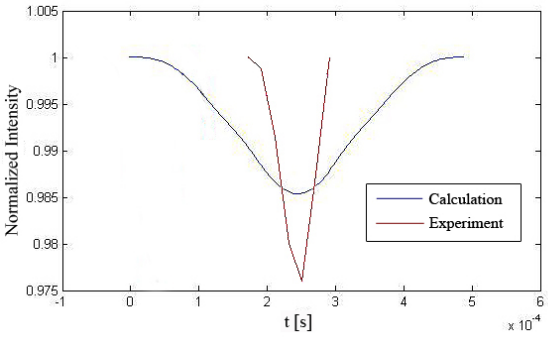

Figure 7: Comparison for a droplet of D_g=264[µm], S_g=4, T_g=T_∞ - simplified model

- The profile of the laser beam was chosen to be Gaussian for the calculation. In reality interference phenomena of the beam with the pinholes and Mie-Scattering on the droplets can be observed.
- This image results from measurements performed at a repetition rate of 80*[kHz]* which corresponds to eight data points per droplet passage at 8.6*[kHz]* injection frequency. Consequently the acquisition rate has been raised up to 250*[kHz]*. The augmentation to 29 points per droplet results in a much smoother curve but enhances also the sensibility towards high-frequency perturbations. The actual Noise correction was therefore improved by adding an adaptable FFT-based band pass filter.

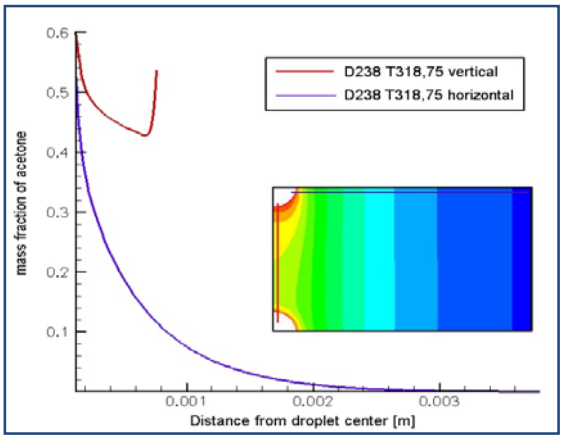

Figure 8: mass fraction profiles from DNS calculation

Application and Discussion of the Refinements

The next step is to change the vapor field model used. For this purpose, the analytically determined field, following equation 5, is replaced by a two-way coupling 2D-DNS calculation, done by B.Frackowiak et al. [7]. This simulation considers the interaction between droplets in a monodisperse stream formation, the widening of the vapor tunnel by the flow of Stephan [10] and the change of the evaporation rate due to the Marangoni effect inside the droplets.

Figure 8 presents the resulting horizontal and vertical vapor mass fraction profiles around a droplet of 238 *[µm]* at a temperature of 318.75 *[K]* situated at 35*[mm]* from the injection. The insert shows the calculated vapor field these profiles are extracted from. This vapor field – after being centered on a droplet and revolved around the axis – will replace the isolated droplet model in the following simulations of vapor absorption.

The horizontal vapor distribution (blue) was confirmed by PLIF measurements until close to the droplet surface using extrapolation of the smoothly rising profile [7]. Because of the blooming effect mentioned above, this was not possible for the vertical distribution. For this reason, the work of the IRE will be focused on matching the vertical profile between the droplets.

A comparison of the advanced model to measurement results is shown in figure 9: The absorption levels for a droplet of 264*[µm]* in diameter at 318.75*[K]* show good coherence. Also the shapes of the two curves are very much closer to

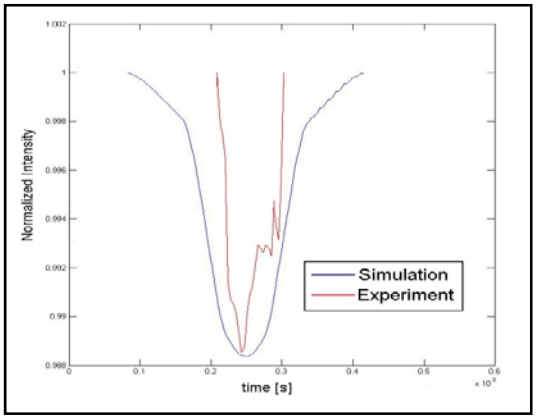

Figure 9: Comparison for a droplet of D_g=264[µm], S_g=4, T_g=318.75[K] - advanced model

each other than this was the case in the comparison to the simplified spherical model. However, the measurement signal shows strong deformations. This indicates that the applied FFT noise correction, which was mentioned above as one of the points of amelioration, is not filtering out all of the perturbing frequencies. Another possible reason for the deformations, interference phenomena between the beams, droplets and optical elements is currently under examination.

Conclusion and Perspectives

A Two-wavelength Infra-Red extinction technique has been applied on a stream of monodisperse droplets. The ability to identify and isolate single droplet passages has been proven. Error sources have been identified; refinements were proposed and partially applied. This lead to a significant improvement in estimating the amplitude and shape of the absorption, caused by a droplet passing the laser beams. However, several difficulties have yet to be resolved until reliable quantitative results of the local concentration values can be obtained: Once quantitative results are available, a comparison to the results of B.Frackowiak, obtained by PLIF, will show synergies and constraints of the two techniques.

Acknowledgement:
This research project has been supported by a Marie Curie Early Stage Research Training Fellowship of the European Community's Sixth Framework Program under contract number MEST-CT-2005-020426.

Nomenclature

c_m	Molar concentration
D_g	Droplet diameter
I	Laser irradiance
I_0	Initial Laser irradiance
$K_{drop\text{-}abs}$	Optical thickness term for drop absorption
$K_{drop\text{-}scat}$	Optical thickness term for drop scattering
K_{vapor}	Optical thickness term for vapor absorption
P	Pressure
S_g	Spacing between droplets
T	Temperature
x,y	Cartesian coordinates
α	Absorption cross section
λ	Wavelength
μ	Mass fraction

References

1. P.C.Ariessohn, S.A.Self and R.H.Eustis, *Applied Optics Vol.19*, 22:3775-3781 (1980).
2. A.R.Chraplyvy, *Applied Optics Vol. 20*, 15: 2620-2624 (1981).
3. P.D.Jennings and J.A.Drallmeier, *Atomization and Sprays*, 6: 537-562 (1996).
4. T.Tsuboi, K.Inomata and Y.Tsunoda, *Japanese Journal of Applied Physics Vol.24*, 1:8-13 (1985).
5. A.E.Klingbeil, *PhD Thesis Stanford University*, Stanford, CA (2007).
6. J.A.Drallmeier, *Applied Optics Vol.33*, 30:7175—7179 (1994).
7. B.Frackowiak, A.Strzelecki and G.Lavergne, *Accepted for Experiments in Fluids*, EIF-0247-2007 (2007).
8. C.Hassa, *LOPOCOTEP Deliverable 4.15*,Cologne, Germany, April 2004.
9. Y.Zhang, T.Yoshizaki and K.Nishida, *Applied Optics Vol.39*, 33: 6221-6229 (2000).
10. W.A Sirignano, *Fluid Dynamics and Transport of Droplets and Sprays*, Cambridge University Press, 1999.